Post-Tensioned Slab-Column Connections

Drift capacity at punching of connections subjected to lateral loading

BY THOMAS H.-K. KANG, JAMES M. LAFAVE, IAN N. ROBERTSON, AND NEIL M. HAWKINS

For buildings in high seismic regions, slab-column frames are commonly used to carry gravity loads. Even though these so-called "nonparticipating" frames are coupled to moment-resisting frames or structural walls designed to resist all of the lateral force demands, it's critical that lateral drift in such a frame doesn't lead to brittle punching shear failures at the slab-column connections.

This issue is currently addressed in ACI 318-05,[1] Section 21.11, "Members not designated as part of the lateral-force-resisting system," which provides a deformation compatibility check as one design criterion. This check places limits on the design story drift ratio, defined as the relative difference of design displacement between the top and bottom of a story divided by the story height. If the specified drift ratio limits are exceeded, a certain amount of shear reinforcement is required in the slab. Alternatively, Section 21.11 allows designers to: 1) simply omit the deformation compatibility check as long as they specify shear reinforcement meeting certain requirements; or 2) demonstrate that the design shear and induced moment at the design story drift can, in fact, be transferred.

Partly based on a database of test results,[2,3] the limit placed on the design story drift is a function of the drift at punching shear failure of a slab-column connection, which is in turn a function of the factored direct shear at the connection and the shear strength of the concrete. More explicitly stated, Section 21.11.5 limits the design story drift ratio to the larger of 0.005 and [0.035 – 0.05 $(V_u/\phi V_c)$], where V_u is the factored gravity load shear force on the slab critical section for two-way action, ϕ is 0.75, and V_c is the nominal concrete shear strength per Section 11.12.2 of ACI 318-05 (Fig. 1).

Subcommittees of ACI Committee 374, Performance-Based Seismic Design of Concrete Buildings, and Joint ACI-ASCE Committee 352, Joints and Connections in Monolithic Concrete Structures, have recompiled and expanded the database of test results and reassessed these data to establish lateral drift limits as a function of the gravity shear ratio[4] $V_u/\phi V_c$, where, for the test data, V_u is the experimentally determined gravity load shear

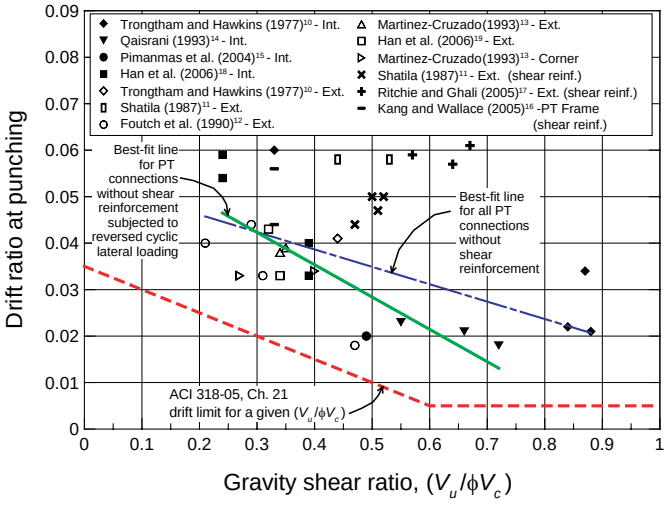

Fig. 1: Drift ratio at punching versus gravity shear ratio for post-tensioned slab-column connections with and without shear reinforcement, where V_c is defined in accordance with ACI 318-05, Eq. (11-36)

force on the slab critical section for two-way action, $\phi = 1.0$, and V_c is calculated per Eq. (11-36) of ACI 318-05.[1] The newly-compiled data set includes test results for more than 70 conventionally reinforced concrete slab-column connection specimens fabricated with and without shear reinforcement,[2,5-8] and it shows that the drift capacity criteria provided in Section 21.11.5 are conservative—only four of 76 test data points fall slightly below the limits specified in ACI 318-05.[8] None of the results in that data set, however, are for post-tensioned slab-column connections.

Given the frequent use of post-tensioned flat plate systems in the U.S., the investigation of the seismic performance of slab-column connections and development of seismic design provisions for nonparticipating frames comprising reinforced concrete (RC) flat plate slabs should be extended to include frames comprising post-tensioned (PT) flat plate slabs. Committee 352 is therefore currently revising ACI 352.1R-89, "Recommendations for Design of Slab-Column Connections in Monolithic Reinforced Concrete Structures,"[9] to address this need (as well as other important new issues). As part of that effort, a committee-sponsored task group has made a detailed review of available research on lateral load tests of slab-column connections with PT slabs, with particular emphasis on their lateral drift capacity as a function of the gravity shear ratio. A summary of that review follows.

SUMMARY OF AVAILABLE RESEARCH

Table 1 summarizes the existing experimental data on lateral load tests of PT slab-column connections. For connections without shear reinforcement, this database includes information on 12 interior, 11 exterior, and two corner connections. For connections with shear reinforcement, the database includes information on seven exterior connections and a two-story, two-bay by two-bay frame.

The tendons in the PT slab specimens were arranged in one of the following three configurations: 1) banded in the lateral loading direction and distributed in the other direction; 2) distributed in the loading direction and banded in the other direction; and 3) distributed in both directions. While the configuration with distributed tendons in both directions was used in the early days of PT slabs, most current construction uses banded tendons. For the few connections subjected to biaxial lateral loading, the tendon layout indicated in Table 1 corresponds to the direction of the first application of lateral loading.

All but one specimen[15] had tendons draped in a parabolic profile and square column cross sections, and in these, two of the tendons were routed through the column cages. The atypical specimen had tendons with a straight profile at the top of the slab placed outside the column cage and a rectangular column cross section that was loaded in the stiff direction.

In all specimens, top reinforcing bars were distributed around the connection per Section 18.9 of ACI 318-05. Bottom bars were provided in nearly 2/3 of the specimens. Nine specimens[10,16,17] had almost equal areas of top and bottom bars. Eleven specimens[12,15,18,19] included bottom bars with less than 2/3 of the area of the top bars.

The $V_u/\phi V_c$ values shown in Table 1 are based on measured material properties. Eighteen of the 33 specimens were tested under a constant gravity load for the duration of the test. For each of the other 15 specimens, the gravity shear force on the connection was increased at specific times during the test. To provide an equal basis for comparison, we've reported only the gravity shear ratio at the time that punching failure occurred.

For all connections in PT slabs, V_c was calculated using the provisions of ACI 318-05, Section 11.12.2.2, where the term V_p was ignored because the angle of tendon inclination was small and tendons were essentially horizontal as they crossed the critical section for shear. The effective depth d used to calculate V_c was taken as the average of the effective depths of the tendons (d_{ps}) or of the bonded bars oriented in the two directions. For exterior connections, d was set equal to d_{ps} for the tendons parallel to the slab edge (tendons perpendicular to the slab edge were vertically centered in the slab). To be consistent with the approach taken by most researchers, the value of $V_u/\phi V_c$ reported in Reference 15 was modified using the average d_{ps} in the two directions rather than the d_{ps} value for the tendons in the loading direction only. The tendon diameters in this reduced-scale specimen were large relative to the slab thickness, so the modified calculation of d_{ps} led to a significant change in $V_u/\phi V_c$—from a reported value of 0.28 to a value of 0.49 in the current database.

For the purposes of this study, the limits of ACI 318-05, Sections 11.12.2.2(a), (b), and (c), respectively concerning the distance from the column perimeter to the slab edge, the square root of the specified compressive strength of the concrete ($\sqrt{f'_c}$), and the compressive stress in the concrete at the centroid of the cross section (f_{pc}), were ignored. Most of the tests were conducted on isolated connection subassemblies (Fig. 2) at approximately 1/2 to 2/3 scale, with the slab edges pin-supported along assumed lateral load inflection points at or near the slab mid-spans (Fig. 2(b) and 2(d)). These isolated specimens had columns extending above and below the slab for a total distance equal to the story height, and the columns were displaced laterally during testing to produce unbalanced moments at the slab-column connections. Other specimens,[10,12] however, represented only small portions of the slab around the column, with the gravity and lateral loads simulated by displacing the slabs (Fig. 2(a) and 2(c)). The slab span lengths l_1 for these specimens were determined based on the actual (scaled-down) prototype buildings used for proportioning and constructing the specimens

TABLE 1:
Post-tensioned slab-column connections subjected to lateral loading

Specimens		Joint type*	Tendon layout†	Gravity loads‡	ϕV_c,§ kips	V_u,‖ kips	$\frac{V_u}{\phi V_c}$	f'_c, psi	f_{pc}, psi	b_o, in.	d, in.	h, in.	l_1,# in.	Lateral loads**	DR,†† %
Trongtham and Hawkins (1977)[10]	S1	Int	B-D	GP	79.6	66.8	0.84	3900	163	73	4.1	5.5	222	RPL	2.2
	S2	Ext	D-D	GP	69.3	30.8	0.44	4200	277	51	4.4	5.5	252	RPL	4.1
	S3	Int	D-B	GP	77.9	67.8	0.87	3698	163	73	4.1	5.5	222	RPL	3.4
	S4	Int	D-D	GP	79.2	69.9	0.88	3800	163	73	4.1	5.5	222	RPL	2.1
	S5	Int	D-D	GP	77.4	25.2	0.33	3596	163	73	4.1	5.5	222	RPL	6.0
Shatila (1987)[11]	S1	Ext	B-D	GP	76.2	40.5	0.53	5188	540	39	4.7	5.9	99	RPL	5.8
	S2‡‡	Ext	B-D	GP	78.4	40.5	0.52	5710	540	39	4.7	5.9	99	RPL	5.0
	S3‡‡	Ext	B-D	GP	81.6	40.5	0.50	6072	570	39	4.7	5.9	99	RPL	5.0
	S4‡‡	Ext	B-D	GP	78.7	40.5	0.51	5783	540	39	4.7	5.9	99	RPL	4.7
	S5§§	Ext	B-D	GP	91.1	40.5	0.44	5986	570	44	4.7	5.9	99	RPL	5.8
	S6‡‡§§	Ext	B-D	GP	86.6	40.5	0.47	5304	550	44	4.7	5.9	99	RPL	4.4
Foutch et al. (1990)[12]	S1	Ext	B-D	GP	61.6	13.0	0.21	7300	450	43	3.3	4.0	168	MTL	4.0
	S2	Ext	B-D	GP	60.8	18.7	0.31	6200	510	43	3.3	4.0	168	MTL	3.3
	S3	Ext	D-B	GP	52.4	15.1	0.29	6100	320	43	3.3	4.0	168	MTL	4.4
	S4	Ext	D-B	GP	55.0	25.6	0.47	7000	315	43	3.3	4.0	168	MTL	1.8
Martinez (1993)[13]	E1	Ext	D-B	CG	25.4	9.0	0.35	4800	199	29	2.9	3.6	144	RCL	3.9
	E2	Ext	B-D	CG	25.2	8.5	0.34	4620	206	29	2.9	3.6	144	RCL	3.8
	C1	Cor	B-D	CG	18.1	7.2	0.40	5890	223	18	2.9	3.6	144	RCL	3.4
	C2	Cor	D-B	CG	18.2	4.9	0.27	6130	211	18	2.9	3.6	144	RCL	3.3
Qaisrani (1993)[14]	I1	Int	D-B	CG	35.6	25.5	0.72	4075	240	43	2.8	3.5	147	RCL	1.8
	I2	Int	D-B	CG	35.6	23.5	0.66	4075	240	43	2.8	3.5	147	RCL	2.1
	I3	Int	D-B	CG	35.6	19.5	0.55	4010	240	43	2.8	3.5	147	RCL	2.3
Pimanmas et al. (2004)[15]		Int	B-D	CG	60.6	29.9	0.49	5858	240	70	2.8	4.7	224	RCL	2.0

Kang and Wallace (2005)[16]	PT Frame‡‡	1st story	B-D	CG	26.0	8.6	0.33	4012	200	41	2.3	3.0	112	RCL	4.4
		2nd story	B-D	CG	26.0	8.6	0.33	4012	200	41	2.3	3.0	112	RCL	5.6
Ritchie and Ghali (2005)[17]	EC3C‡‡	Ext	B-D	CG	36.9	24.7	0.67	3741	58	38	4.2	5.9	95	RCL	6.1
	EC5C‡‡	Ext	B-D	CG	38.6	24.7	0.64	3712	95	38	4.2	5.9	95	RCL	5.7
	EC9C‡‡	Ext	B-D	CG	43.4	24.7	0.57	4089	160	38	4.2	5.9	95	RCL	5.9
Han et al. (2006)[18]	PI-B50	Int	B-D	CG	77.1	29.7	0.39	4684	175	64	4.1	5.1	189	RCL	3.3
	PI-B30	Int	B-D	CG	77.1	18.2	0.24	4684	175	64	4.1	5.1	189	RCL	5.9
	PI-D50	Int	D-B	CG	77.1	29.7	0.39	4684	175	64	4.1	5.1	189	RCL	4.0
	PI-D30	Int	D-B	CG	77.1	18.2	0.24	4684	175	64	4.1	5.1	189	RCL	5.4
Han et al. (2006)[19]	PE-B50	Ext	B-D	CG	55.7	18.9	0.34	4684	175	44	4.3	5.1	189	RCL	3.3
	PE-D50	Ext	D-B	CG	55.7	18.0	0.32	4684	175	44	4.3	5.1	189	RCL	4.3

Note: 1 in. = 25.4 mm; 1 kip = 4.45 kN; 1 psi = 0.0069 MPa.

* Int = interior; Ext = exterior; Cor = corner.

† B-D = banded tendons in the lateral loading direction and distributed tendons in the other direction; D-B = distributed tendons in the loading direction with banded tendons in the other direction; D-D = distributed tendons in both directions.

‡ GP = gravity shear ratio at punching; CG = constant gravity load.

§ ϕV_c = shear strength for test connection, calculated with $\phi = 1.0$ and using V_c per Eq. (11-36) of ACI 318-05.[1]

|| V_u = gravity load shear force on the test slab critical section for two-way action.

# Indicates slab span length of scaled-down prototype.

** MTL = monotonic lateral loading; RPL = repeated lateral loading; RCL = reversed cyclic lateral loading.

†† DR = drift ratio at punching (for negative bending at exterior and corner connections).

Ext connections tested by Trongtham and Hawkins (1977)[10] and Foutch et al. (1990)[12]

$DR = \Delta_a / l$ per Fig. 2(a) and 2(c), respectively.

Int connections tested by Trongtham and Hawkins (1977)[10]

$DR = \frac{1}{2}(\Delta_a / l + \Delta_b / l)$ per Fig. 2(a).

Connections tested by Shatila (1987)[11]

$DR = \Delta_a / l_a$ per Fig. 2(b).

Connections tested by Ritchie and Ghali (2005)[17]

$DR = \Delta / l$ per Fig. 2(b).

Connections tested by Qaisrani (1993),[14] Martinez-Cruzado (1993),[13] Pimanmas et al. (2004),[15] and Han et al. (2006)[18,19]

$DR = \Delta / l$ per Fig. 2(d).

Connections by Kang and Wallace (2005)[16]

$DR = \frac{1}{2}(\Delta_a / l_a + \Delta_b / l_b)$ for 1st floor connections and $DR = \Delta_b / l_b$ for 2nd floor connections per Fig. 2(e).

‡‡ Indicates specimens with shear reinforcement.

§§ Exterior connections with cantilevered slab overhangs.

and are reported in Table 1. The ratio of the slab span length (center-to-center of columns) to the slab thickness (l_1/h) for most of the specimens ranged between 35 and 48, which are typical of values used for post-tensioned flat plate construction in the U.S. The specimens shown in Fig. 2(b),[11,17] however, had a significantly lower span-to-thickness ratio. Using the assumption that the inflection points would occur near the slab mid-spans, l_1/h for this slab was 15—this ratio is more representative of a flat plate frame comprising the primary lateral-force-resisting system in regions of moderate seismic risk.

As shown in Fig. 2, a variety of loading and boundary condition schemes were used in the tests. The types of lateral loads applied to the specimens were classified into three categories—monotonic lateral loading, repeated lateral loading, and reversed cyclic lateral loading. The specimens tested under repeated lateral loads were cycled several times but in the same bending direction. The two-story by two-bay frame[16] was tested using a shake table to simulate earthquake actions (Fig. 2(e)), while the specimens reported in References 13 and 14 (Fig. 2(d)) were subjected to clover-leaf patterns of biaxial lateral drift. The lateral loads for both of these studies were categorized as reversed cyclic lateral loading.

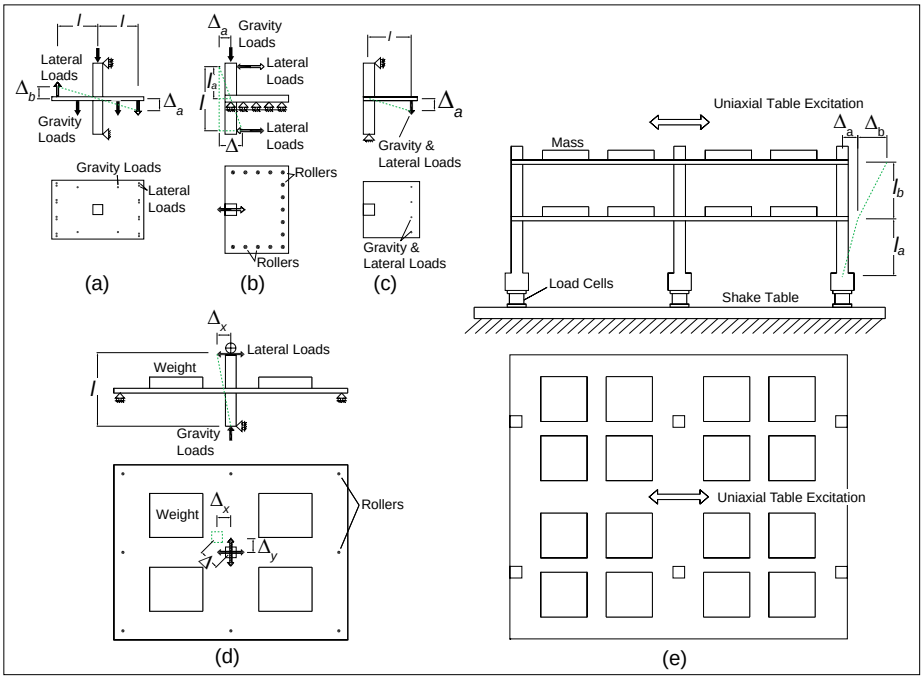

Fig. 2: Typical test configurations (scaled to have the same story height): (a) Trongtham and Hawkins (1977)[10]; (b) Shatila (1987)[11] and Ritchie and Ghali (2005)[17]; (c) Foutch et al. (1990)[12]; (d) Martinez-Cruzado (1993)[13], Qaisrani (1993)[14], Pimanmas et al. (2004)[15], and Han et al. (2006)[18,19]; and (e) Kang and Wallace (2005)[16]

DRIFT CAPACITY AT PUNCHING VERSUS GRAVITY SHEAR RATIO

The average specimen drift ratio at punching was calculated (Fig. 2 and Table 1) and plotted as a function of gravity shear ratio for each of the test results (33 specimens) (Fig. 1). The data indicate that, as is the case for RC slab connections, the drift ratio at punching for PT slab-column connections is strongly influenced by the gravity shear ratio. Figure 1 further shows that the ACI 318-05 Section 21.11.5 requirement for use of shear reinforcement in slab-column connections as part of nonparticipating frames is conservative for PT slab connections (as has previously also been noted for RC slab connections).[2,5-8] The influence of gravity shear ratio is especially evident for connections tested within a specific test program. The best-fit lines in Fig. 3 were derived from a database of RC and PT slab specimens without shear reinforcement,[8] using a linear least-squares fit method. The best-fit lines suggest that PT slab-column connections without shear reinforcement

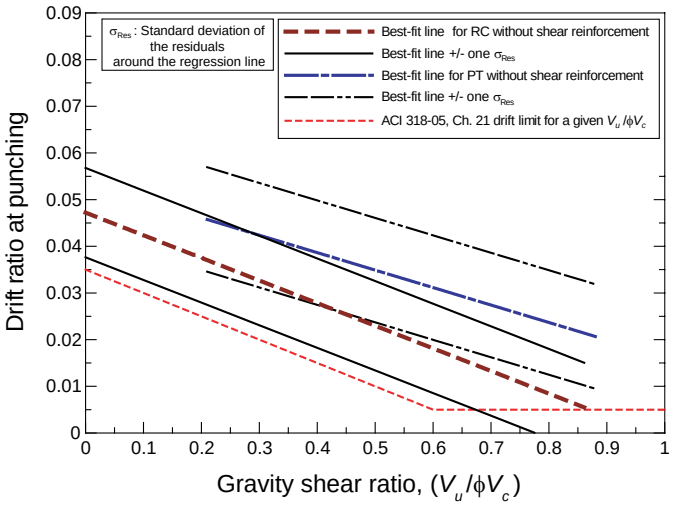

Fig. 3: Best-fit lines and confidence bands for conventionally reinforced and post-tensioned slab-column connections, where V_c is defined in accordance with ACI 318-05, Eq. (11-33) through (11-36)

can sustain higher drift ratios prior to punching than comparable RC slabs under a variety of loading types. In part, the higher drift ratios may be due to the larger l_1/h values used in PT slab construction—l_1/h values are about 40 and 25 for PT and RC slabs, respectively—that make PT slabs more flexible than RC slabs. The higher

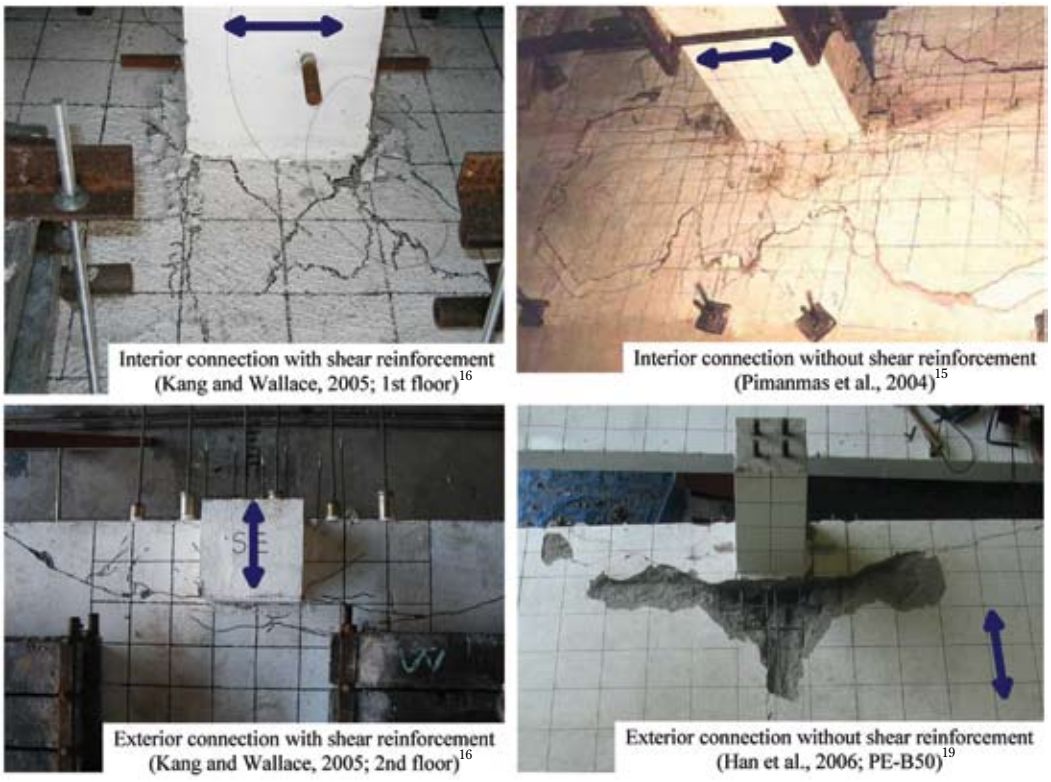

Fig. 4: Observed punching damage after the tests (arrows indicate testing directions)

drift ratios are also likely due to the roughly 5 to 15% increase in shear strength at the connection of PT slabs relative to RC slabs attributable to the in-plane f_{pc} (generally 150 to 250 psi [1.03 to 1.72 MPa]).[8]

The results shown in Fig. 1 also indicate that the loading conditions for the PT slab specimens without shear reinforcement affected the drift ratio at punching. The best-fit line for the 14 PT slab specimens subjected to reversed cyclic loads indicates lower drift ratios than the trend line for all specimens. Although some test results[18,19] indicate that slabs with distributed tendons have different drift capacities at punching than slabs with banded tendons, no significant differences in drift capacities at punching were noted as a function of the tendon arrangement across all PT specimens. Further, because the PT data are limited, no distinction can currently be made between the drift capacities for interior versus exterior connections. Similarly, no such distinction with regard to connection type is currently made in ACI 318-05, Section 21.11.5, even though some test data for RC slab connections[3] show that drift ratios at punching are higher for exterior than interior connections.

As seen in Fig. 1, drift ratios at punching were observed to be larger for isolated PT exterior connections with shear reinforcement[17] than for those without shear reinforcement.[13,19] This result is probably due to the large strain ductility provided by yielding of the shear reinforcement. A seemingly contrary result, however, was seen in one test program.[11] As mentioned earlier, however, these specimens were proportioned to represent relatively low slab l_1/h values on the order of about 15. Further, because they used rollers along all three edges of the slab (Fig. 2(b)), the deformed shape of the slab across its width would have been inconsistent with that in an actual building. Such test configurations therefore tend to induce larger slab shear-to-moment ratios at the slab-column interfaces than for typical flat plate geometric and boundary conditions (compare Fig. 2(b) versus 2(d) or 2(e)). Thus, these results may not be appropriate for direct comparison with other test results.

The range of drift ratios at punching observed for the PT flat plate frames with shear reinforcement[16] is close to the best-fit obtained from isolated PT slab connections without shear reinforcement, as indicated in Table 1 and Fig. 1. Use of shear reinforcement, however, significantly reduced the extent of punching damage and the shear strength degradation after punching, as can be seen in Fig. 4. While most of the specimens without shear reinforcement[13-15,18,19] exhibited sudden punching failures that led to residual strengths that were typically only 10% of the peak lateral load capacity, specimens with shear reinforcement[16,17] exhibited only gradual strength degradation after reaching the peak lateral load. Residual strengths of the latter were often greater than 60% of the

peak lateral load capacity, even after several post-punching load cycles to increasing drift ratios.

Bottom reinforcing bars did not appear to significantly affect the drift ratio at punching; however, the hysteretic energy dissipation capacity appeared to be affected. For the PT slab connections without bottom bars,[13,14] only limited hysteretic behavior was exhibited, whereas the connections with bottom bars showed better seismic performance including considerable bottom bar yielding.[16] Other studies[18,19] have investigated the need for and the required quantity of bottom bars for PT slab connections. Those test data indicate that moment reversal occurred at drift ratios of about 0.5% and that bottom structural integrity reinforcement, placed according to ACI 318-05, Section 7.13.2.5, and ACI 352.1R-89,[9] Section 5.3, yielded at drift ratios of between 2.2 and 3.5%. Based on these results, we believe that bonded bottom reinforcement per Section 7.13.2.5 is desirable for post-tensioned connections of nonparticipating frames where moment reversal is likely to occur.

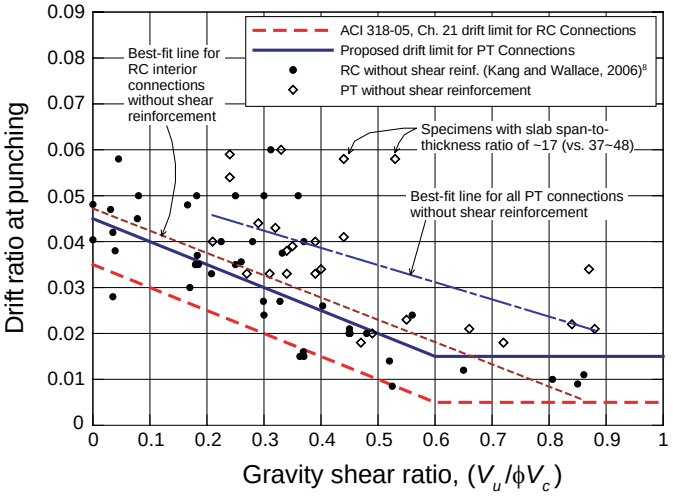

Fig. 5: Comparison of drift ratio limits with conventionally reinforced and post-tensioned slab-column connection test data, where V_c is defined in accordance with ACI 318-05, Eq. (11-33) through (11-36)

RECOMMENDATIONS

Based on the review presented in this article, a new bilinear drift ratio limit illustrated in Fig. 5 and equal to the larger of 0.015 and $[0.045 - 0.05V_u/\phi V_c]$ is proposed for post-tensioned slab-column connections. Above this limit, the use of shear reinforcement in PT slab-column connections should be required in nonparticipating frames.

The new limit is a lower bound estimate of the drift ratio at punching shear failure for all gravity shear ratios and tested connection types and takes into account the differences in the need for shear reinforcement between conventionally reinforced and post-tensioned connections. Only two of the 33 PT slab test results fall slightly below the new limit. When the design story drift ratio exceeds the drift ratio limit, the test results show that shear reinforcement should be provided such that its strength V_s is not less than the current minimum per ACI 318-05, Section 21.11.5. Tests[11,16,17] of PT slab-column connections with shear reinforcement extended a minimum of 1.9h, 2.25h, and 2.8h from the column face demonstrated excellent performance. Therefore, it is proposed that the current requirement that shear reinforcement extend 4h from the face of the support be reduced to 3h for PT slab connections.

Based on the experimental data shown in Fig. 5, the maximum allowable factored gravity shear force for PT connections that are part of intermediate moment frames (given in ACI 318-05, Section 21.12.6.8) can be increased from the current $0.4\phi V_c$ to $0.6\phi V_c$. Further, this limitation could be waived if shear reinforcement is provided and the eccentric shear stress due to unbalanced moment does not exceed $0.5\phi v_n$, or if the story drift ratio does not exceed the drift limit proposed in the preceding paragraph, where v_n is the nominal shear strength of the slab-column connection as defined by ACI 318-05, Section 11.12.6.2.

Finally, while the limits of ACI 318-05 Section 11.12.2.2 (a), (b), and (c) were ignored in developing the recommendations of this article, it appears advisable, based on the reported behavior of the test specimens, that the design f_{pc} value should be between 125 and 500 psi (0.9 and 3.5 MPa) and that the expression for V_c in Eq. (11-36) be applicable to exterior connections provided that at least two tendons pass through the column core, they are normal to the discontinuous edge, and the remaining tendons in that direction are uniformly distributed across the width of the slab.

Acknowledgments

The authors would like to thank other members of Joint ACI-ASCE Committee 352, Joints and Connections in Monolithic Concrete Structures, for their constructive comments and suggestions regarding the subject of this article.

References

1. ACI Committee 318, "Building Code Requirements for Structural Concrete (ACI 318-05) and Commentary (318R-05)," American Concrete Institute, Farmington Hills, MI, 2005, 430 pp.

2. Moehle, J.P., "Seismic Design Considerations for Flat-Plate Construction," *Mete A. Sozen Symposium...A Tribute From His Students* (SP-162), J.K. Wight and M.E. Kreger, eds., American Concrete Institute, Farmington Hills, MI, 1996, pp. 1-34.

3. Megally, S., and Ghali, A., "Punching Shear Design of Earthquake-Resistant Slab-Column Connections," *ACI Structural Journal*, V. 97, No. 5, Sept.-Oct. 2000, pp. 720-730.

4. Hueste, M.B.D.; Lepage, A.; Browning, J.P.; and Wallace, J.W., "Performance-Based Seismic Design Criteria for Slab-Column Connections," *ACI Structural Journal* (accepted for publication).

5. Pan, A.D., and Moehle, J.P., "Lateral Displacement Ductility of Reinforced Concrete Flat Plates," *ACI Structural Journal*, V. 86, No. 3, May-June 1989, pp. 250-258.

6. Hueste, M.B.D., and Wight, J.K., "Nonlinear Punching Shear Failure Model for Interior Slab-Column Connections," *Journal of Structural Engineering*, V. 125, No. 9, Sep. 1999, pp. 997-1008.

7. Robertson, I.N.; Kawai, T.; Lee, J.; and Enomoto, B., "Cyclic Testing of Slab-Column Connections with Shear Reinforcement," *ACI Structural Journal*, V. 99, No. 5, Sept.-Oct. 2002, pp. 605-613.

8. Kang, T.H.-K., and Wallace, J.W., "Punching of Reinforced and Post-Tensioned Concrete Slab-Column Connections," *ACI Structural Journal*, V. 103, No. 4, July-Aug. 2006, pp. 531-540.

9. Joint ACI-ASCE Committee 352, "Recommendations for Design of Slab-Column Connections in Monolithic Reinforced Concrete Structures (ACI 352.1R-89) (Reapproved 2004)," American Concrete Institute, Farmington Hills, MI, 2004, 22 pp.

10. Trongtham, N., and Hawkins, N.M., "Moment Transfer to Columns in Unbonded Post-Tensioned Prestressed Concrete Slabs," *Report* SM77-3, Department of Civil Engineering, University of Washington-Seattle, Seattle, WA, 1977, 186 pp.

11. Shatila, M., "Prestressed Concrete Slab-Edge Column Connection with Stud Shear Reinforcement," MSc thesis, Department of Civil Engineering, University of Calgary, Calgary, AB, Canada, 1987, 203 pp.

12. Foutch, D.A.; Gamble, W.L.; and Sunidja, H., "Tests of Post-Tensioned Concrete Slab-Edge Column Connections," *ACI Structural Journal*, V. 87, No. 2, Mar.-Apr. 1990, pp. 167-179.

13. Martinez-Cruzado, J.A., "Experimental Study of Post-Tensioned Flat Plate Exterior Slab-Column Connections Subjected to Gravity and Biaxial Loading," PhD thesis, Department of Civil Engineering, University of California, Berkeley, CA, 1993, 378 pp.

14. Qaisrani, A.-N., "Interior Post-Tensioned Flat-Plate Connections Subjected to Vertical and Biaxial Lateral Loading," PhD thesis, Department of Civil Engineering, University of California-Berkeley, Berkeley, CA, 1993, 303 pp.

15. Pimanmas, A.; Warnitchai, P.; and Pongpornsup, S., "Seismic Performance of 3/5 Scaled Post-tensioned Interior Flat Slab-Column Connections," *Proceedings of the Asia Conference on Earthquake Engineering 2004*, Manila, Philippines, Mar. 2004, 9 pp.

16. Kang, T.H.-K., and Wallace, J.W., "Dynamic Responses of Flat Plate Systems with Shear Reinforcement," *ACI Structural Journal*, V. 102, No. 5, Sept.-Oct. 2005, pp. 763-773.

17. Ritchie, M., and Ghali, A., "Seismic-Resistant Connections of Edge Columns with Prestressed Slabs," *ACI Structural Journal*, V. 102, No. 2, Mar.-Apr. 2005, pp. 314-323.

18. Han, S.W.; Kee, S.-H.; Kang, T.H.-K.; Ha, S.-S.; Wallace, J.W.; and Lee, L.-H., "Cyclic Behavior of Interior Post-Tensioned Flat Plate Connections," *Magazine of Concrete Research*, Telford, V. 58, No. 10, Dec. 2006, pp. 699-711.

19. Han, S.W.; Kee, S.-H.; Park, Y.-M.; Lee, L.-H.; and Kang, T.H.-K., "Hysteretic Behavior of Exterior Post-Tensioned Flat Plate Connections," *Engineering Structures*, V. 28, No. 14, Dec. 2006, pp. 1983-1996.

Received and reviewed under Institute publication policies.

ACI member **Thomas H.-K. Kang** has been a Lecturer for many courses, including prestressed concrete design and the behavior of reinforced concrete elements, at the University of California at Los Angeles, where he received his PhD, and has conducted major research and consulting projects in California. He is the Secretary of Joint ACI-ASCE Committee 352, Joints and Connections in Monolithic Concrete Structures, and is a professional member of the Post-Tensioning Institute.

ACI member **James M. LaFave** is an Associate Professor of Civil Engineering at the University of Illinois at Urbana-Champaign and a licensed Professional Engineer. He is the Chair of Joint ACI-ASCE Committee 352, Joints and Connections in Monolithic Concrete Structures, and is a member of ACI Committees 374, Performance-Based Seismic Design of Concrete Buildings; 439, Steel Reinforcement; and E802, Teaching Methods and Educational Materials.

ACI member **Ian N. Robertson** is a Professor of Civil Engineering at the University of Hawaii at Manoa. He is a member of Joint ACI-ASCE Committee 352, Joints and Connections in Monolithic Concrete Structures, and a member of ACI Committee 209, Creep and Shrinkage in Concrete.

Neil M. Hawkins, FACI, is a Professor Emeritus of Civil Engineering at the University of Illinois at Urbana-Champaign. He is a member of ACI Committee 318, Structural Concrete Building Code, where he chairs the Task Group on Seismic Design of Piles, and is a member of the subcommittees on Shear and Seismic Design. He is also a member of ACI Committees 215, Fatigue of Concrete; 408, Bond and Development of Reinforcement; 446, Fracture Mechanics; ITG-5, Precast Shear Walls for High Seismic Applications; and Joint ACI-ASCE Committees 445, Shear and Torsion, and 550, Precast Concrete Structures.